Analysis of the NbC(111)-($\sqrt{3}\times\sqrt{3}$)R 30°-Al surface structure by impact-collision ion-scattering spectroscopy

Wataru Hayami, Ryutaro Souda, Takashi Aizawa, Shigeki Otani, and Yoshio Ishizawa
National Institute for Research in Inorganic Materials, 1-1 Namiki, Tsukuba, Ibaraki 305, Japan
(Received 30 October 1992; revised manuscript received 11 January 1993)

The structure of the NbC(111) clean surface and the aluminum adsorption system at room temperature have been studied by impact-collision ion-scattering spectroscopy, reflection high-energy electron diffraction (RHEED), low-energy electron diffraction, and computer simulation. It has been found that the clean surface exhibits a 1×1 RHEED pattern and no reconstruction occurs. The outermost layer consists of Nb atoms and relaxes inward by 0.20±0.05 Å, which is equal to 15.5±3.9% of the space between the first and second layers of the bulk. The carbon atoms in the second layer also shift inward by 0.05±0.05 Å. The Al-adsorbed surface has a ($\sqrt{3}\times\sqrt{3}$)R30° structure with slight modulation. The Al atoms occupy two-thirds of the threefold-hollow sites, under which a Nb atom of the third layer is situated. Adsorbed Al atoms make a honeycomb pattern. The distance between the Al atom and the surface has been determined to be 2.25±0.05 Å. The Al-Nb bond length is 2.90±0.05 Å.

I. INTRODUCTION

Transition-metal carbides (TMC's) have been studied for years because they have unusual properties such as a high melting point, large hardness, brittleness, and metallic conductivity.[1,2] The crystal structure of group-IV and group-V TMC's is a NaCl type as shown in Fig. 1. According to theoretical investigations,[3–9] it has been revealed that the metal-carbon bonding in TMC's has features of covalent-, ionic-, and metallic-type bonds simultaneously. This complicated nature of bonding is the origin of their properties. With respect to their application as a material, their use for the wall of a nuclear fusion reactor,[10] for a field electron emitter,[11] and for a catalyst,[12] etc., has been suggested. Recently, monolayer graphite produced on the TMC surface by the thermal chemical vapor deposition method has been reported.[13,14] This offers a new possibility for TMC's as a catalyst and a substrate for thin films. Therefore, fundamental studies of the surfaces are of interest and many experiments have been performed so far.

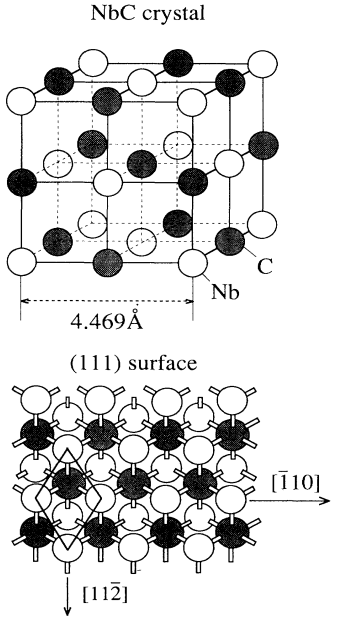

FIG. 1. Crystal structure of NbC and its (111) surface. The (111) surface is terminated by Nb atoms (see text).

Among the group-V TMC's (VC, NbC, TaC), VC_x has a little different nature from the other two in that carbon vacancies are arranged with long-range order. Studies of the $VC_{0.8}$(111) surface by scanning tunneling microscopy[15] and the V_6C_5(111) surface by ion-scattering spectroscopy (ISS) and x-ray photoelectron spectroscopy[16] (XPS) have been reported. The atomic structure of the TaC(100) surface has been studied by low-energy electron diffraction (LEED) and uv photoelectron spectroscopy (UPS).[17] As for NbC, the (100) surface[18] and (100), (111) surfaces with O_2, CO, CH_3OH adsorption[19] have been studied by UPS.

There are few studies about metal-atom adsorption on TMC surfaces. In the present work, Al has been chosen as an adsorbate to compare with the result of gas (O_2, D_2, N_2) adsorption. The surface structure has been quantitatively investigated by impact-collision ion-scattering spectroscopy (ICISS) and computer simulation.

II. EXPERIMENT

A. Sample preparation

A single-crystal rod of NbC_x was prepared by the floating-zone method.[20] The dimension of the rod was 8 mm in diameter and 100 mm in length. The value of x is 0.95 and the lattice constant is 4.469 Å. The rod was oriented toward the [111] direction within 1° by the usual x-ray Laue method and the sample of 1 mm thickness was cut off by a spark erosion cutter. The sample was

mechanically polished to a mirror surface with B_4C powder and diamond paste. Generally, the surfaces of the group-IV and group-V TMC's are stable compared with ordinary metals, and the NbC(111) clean surface can be obtained simply by heating at 2200 °C by means of electron bombardment under a pressure of 10^{-10} Torr. A sharp reflection high-energy electron (RHEED) pattern was observed and the cleanliness of the surface was confirmed by ISS using 1-keV He^+ ions which are sensitive to contamination on the surface.

B. Instrument

ICISS measurements were performed in a stainless-steel ultrahigh-vacuum chamber pumped by polyphenylether diffusion and titanium sublimation pumps. The base pressure was 2×10^{-10} Torr. The chamber is equipped with a He^+ ion gun, a Li^+ ion gun, and RHEED or LEED optics. A 150° spherical-sector electrostatic analyzer was set in the chamber for the energy analysis of both ions and electrons. Both ion guns were differentially pumped so that the pressure inside the main chamber remained below 5×10^{-10} Torr during the ICISS experiment.

C. ICISS principle

The principle of ICISS is described in detail in Ref. 21. It is known that the Thomas-Fermi-Moliére potential[22] is appropriate for the energy region of ICISS, and is expressed by the formula

$$V(r)=f\left[\frac{r}{a}\right]\frac{Z_1Z_2e^2}{r}\ , \tag{1}$$

$$f(x)=0.35\exp(-0.3x)+0.5\exp(-1.2x)+0.10\exp(-6.0x)\ , \tag{2}$$

$$a=Ca_F=C0.8853a_B(Z_1^{1/2}+Z_2^{1/2})^{-2/3}\ , \tag{3}$$

where Z_1, Z_2 are the atomic numbers of the projectile ion and target atom, respectively, a_F is the screening length proposed by Firsov,[23] C is a factor for adjusting a_F to the experimental value, and a_B is the Bohr radius.

The Li^+ ion beam was mainly used for ICISS measurements because its small neutralization probability makes it possible to get the information not only about the outermost layer but also about the several underlayers. The damage of the surface caused by Li^+ ions during the experiment is negligible since the current density of the beam and the time required for one ICISS spectrum is only a few nA/mm^2 and 3 min, respectively.

III. RESULTS AND DISCUSSION

A. Clean surface

After heating at 2200 °C under a pressure in the 10^{-10}-Torr range, the sample exhibits a sharp 1×1 RHEED pattern and neither reconstruction nor facets occur. Figure 2 shows ISS data for the clean surface. A He^+ ion has a tendency to be neutralized at solid surfaces because

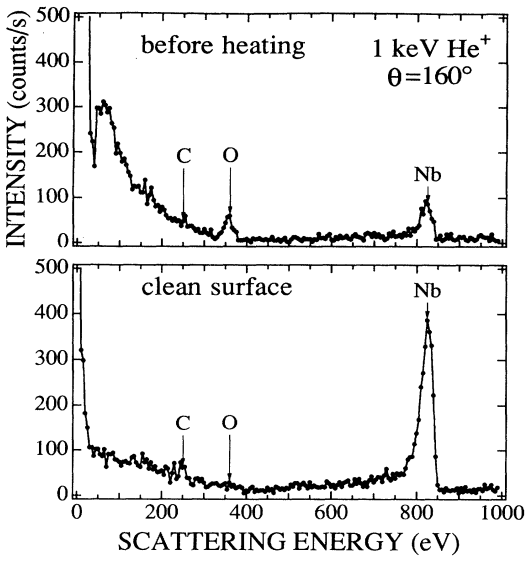

FIG. 2. He^+ ISS spectrum of the NbC(111) surface. The incident angle is 80° from the surface plane and the beam azimuthal direction is [11$\bar{2}$].

of its large ionization potential and ions penetrating into the bulk are neutralized almost 100%. Therefore, ISS using He^+ ions is sensitive to the composition of the outermost layer. While the Nb peak increases after heating, the C and O peaks decrease to nearly zero. This indicates that the NbC(111) clean surface is terminated by Nb atoms. Termination by metal atoms is a common character seen in the (111) surface of group-IV and group-V TMC's.

Figure 3 shows the ISS spectrum using a 1-keV Li^+ ion beam. A peak corresponding to a Nb atom can be seen but peaks for the other lighter elements (C, O, etc.) are buried in the background. The high level of the background results from the fact that the neutralization probability of a Li^+ ion is so small that Li^+ ions inelastically scattered in the bulk can be detected. The ICISS measurements have been performed with respect to the Nb

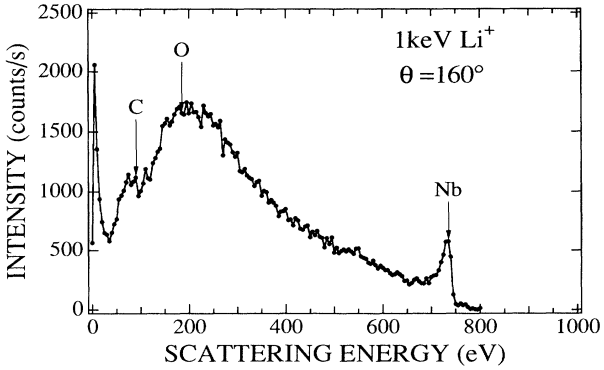

FIG. 3. Li^+ ISS spectrum of the NbC(111) clean surface. The incident angle is 80° from the surface plane and the beam azimuthal direction is [11$\bar{2}$].

peak.

Figure 4 shows the ICISS spectrum of the NbC(111) clean surface. The azimuthal direction of the incident beam is [11$\bar{2}$]. All the ICISS spectra in this work were measured using a 1-keV Li^+ ion beam, and the scattering angle θ was fixed at 160° in the laboratory system. The horizontal axis and vertical axis correspond to the incident angle measured from the surface, and the Li^+ ion intensity backscattered from Nb atoms, respectively. In the spectrum in Fig. 3, two shadowing features (marked with *s*) and one blocking feature (marked with *b*) are observed. The configuration of atoms is illustrated below. The first shadowing at 13.9° is attributed to that of the first-layer Nb [hereafter referred to as Nb(1)] over Nb(1). The second one at 52.0° results from the shadowing of the second-layer C [referred to as C(2)] over the third-layer Nb [referred to as Nb(3)]. At the angle near 52°, the shadowing of Nb(1) over Nb(3) is likely to occur. However, on careful examination, it is found that the critical angle of Nb(1)-Nb(3) shadowing is a little smaller than 52° (about 50°), and then the Nb(3) atom is still in the shadowcone of C(2). Therefore, the shadowing feature of the Nb(1)-Nb(3) pair cannot appear in the spectrum. The shadowcone of Nb(1) over Nb(3) is omitted from the figure. The cause of the blocking effect arising at 81.4° is that the Nb(1) atom obstructs outgoing Li^+ ions scattered by the Nb(3) atom.

To determine the configuration of atoms precisely, computer simulations were performed on the basis of the three-atom model. The method is fundamentally the same as the two-atom model devised by Williams *et al.*[24] Under a condition that the scattering angle is 160°, a phenomenon called self-blocking effect never occurs, but blocking effects by the third atom must be taken into account. Therefore, we consider the process of three sequential scattering events by three atoms (Fig. 5), and calculate a differential cross section. Parameters involved in the calculation are those related to the configuration of atoms and the Firsov length mentioned before. The factor C multiplying the Firsov length for Nb can be experimentally determined to be 0.85 from the ICISS spectra in two different azimuths. There exists some arbitrariness in the factor for the C and Al atoms. It is said that the factor is expressed by the formula[25]

$$C = 0.69 \pm 0.0051(Z_1 + Z_2)\,, \tag{4}$$

where Z_1 and Z_2 are the atomic numbers of the projectile and target atoms. The formula seems to be in good agreement with experiment although there is some disagreement which depends on the experimental conditions (beam energy, neutralization probability, etc.). Since the difference of the experimental values from the formula is almost systematic from one element to another,[26] we estimated the factors for C and Al by multiplying the formula by 0.85/0.91 (0.85 and 0.91 are the experimental value and the calculated value from the formula for Nb, respectively). Consequently, the factors for C and Al are assumed to be 0.69 and 0.72, respectively. This estimation will give a sufficient accuracy for our purpose because even if the factor deviates from the real value by 0.1, the error of the position of the atoms does not exceed ±0.05 Å.

Once the Firsov length factors are determined, the remaining unknown parameters are those related to the three-atom configuration. Each atom is moved step by step in order to make a calculation curve fit to the experimental data. The solid line in Fig. 4 is the best-fitted

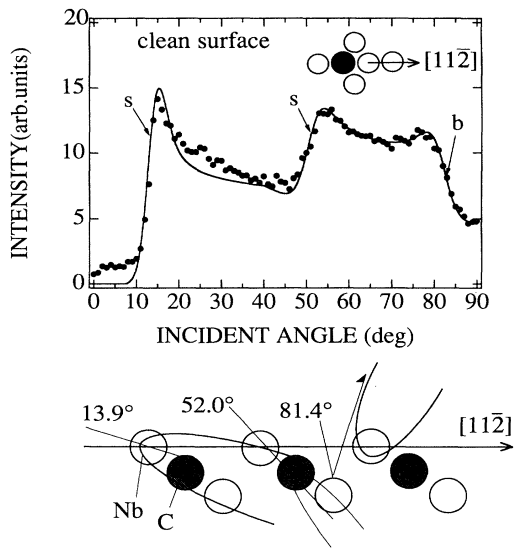

FIG. 4. ICISS spectrum of the NbC(111) clean surface. Solid circles are the experimental data and the solid line is the calculation. *s* means shadowing effect and *b* means blocking effect. The inseted figure shows the top view of the surface unit cell and beam direction. A side view of the surface is given below.

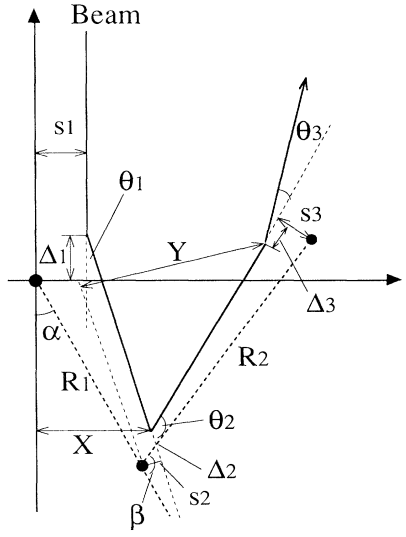

$$\theta = \theta_1 + \theta_2 + \theta_3 = 160°$$

FIG. 5. Schematic diagram of the three-atom scattering process. The total scattering angle is fixed at 160°. Details for the method of calculation are given in Ref. 24.

curve, from which it is found that the Nb(1) and C(2) atoms relax inward by 0.20±0.05 and 0.05±0.05 Å, respectively. 0.20 Å corresponds to 15.5±3.9% of the distance between the first and second layer of the bulk, and is almost the same as for the HfC(111) surface.[27]

Figure 6 shows the ICISS spectrum measured in the [$\bar{1}\,\bar{1}$2] azimuth. At a glance, two shadowing peaks are conspicuous. These peaks are explained as illustrated below. The first shadowing at 13.9° results from the same atom pair as in the [11$\bar{2}$] direction. The second one at 74.5° is assumed to be the shadowing of Nb(1) over Nb(3). The shadowing of C(2) over Nb(3) does not appear in the spectrum because at the critical angle of C(2)-Nb(3) shadowing, Li ions scattered by Nb(3) are obstructed by Nb(1) and are not detected. The shadowcone of C(2) over Nb(3) is omitted from the figure. By comparing the experimental data with computer simulations, it is concluded that Nb(1) atoms relax inward by 0.20±0.05 Å. This value completely agrees with the result obtained in the [11$\bar{2}$] direction.

Figure 7 shows the ICISS spectrum in the [$\bar{1}$10] azimuth. Two shadowing peaks are observed but the second one around 70° is broad. The first shadowing peak at 21.2° is attributed to that of a Nb(1)-Nb(1) pair. The reason why the second peak is broad is that the Nb(3) atoms are hidden by the shadowcone of the Nb(1) atoms obliquely. In other words, the Nb(3) atoms are out of the scattering plane of the Nb(1) atoms. In such a situation, a three-atom model is not applicable for the calculation. The ICISS data in the [$\bar{1}$10] azimuth do not contradict the results of the [11$\bar{2}$] and [$\bar{1}\,\bar{1}$2] azimuths.

In summary, the NbC(111) clean surface is terminated by a Nb layer, where Nb(1) and C(2) relax inward by 0.20±0.05 and 0.05±0.05 Å, respectively.

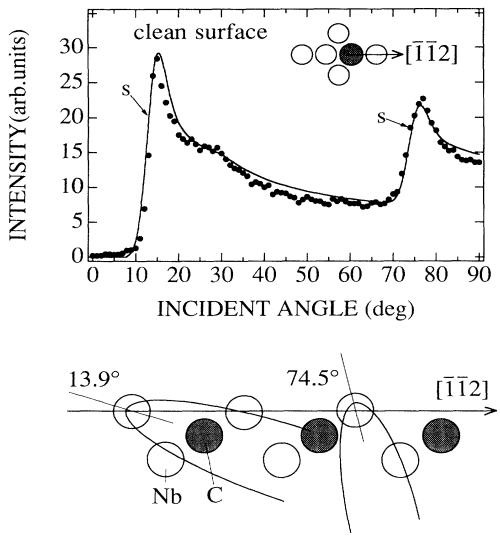

FIG. 6. ICISS spectrum of the NbC(111) clean surface. Solid circles are the experimental data and the solid line is the calculation. *s* means shadowing effect.

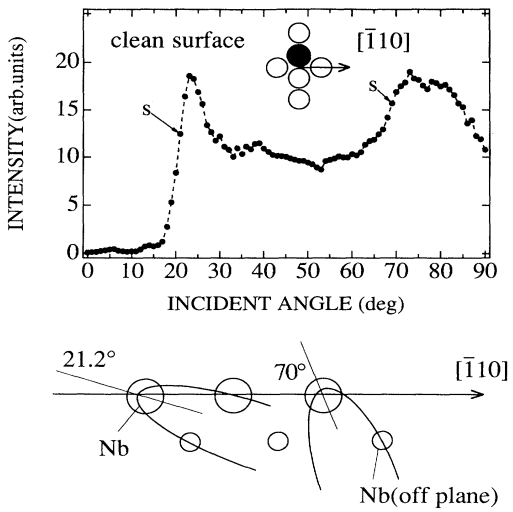

FIG. 7. ICISS spectrum of the NbC(111) clean surface. Solid circles are the experimental data. The dashed line is a guide for the eye. *s* means shadowing effect.

B. Al-adsorbed surface

Al was deposited on the NbC(111) clean surface at room temperature. During deposition, incommensurate spots gradually appeared in the RHEED pattern. After saturation, the sample was heated up to 900 °C, then the RHEED pattern came to exhibit a ($\sqrt{3}\times\sqrt{3}$)R30° structure. This structure was investigated by ICISS using a 1-keV Li^+ ion beam.

Figure 8 shows the ICISS spectrum in the [$\bar{1}$10] direction. The horizontal axis and vertical axis correspond to the incident angle measured from the surface, and the Li^+ ion intensity backscattered from Nb atoms, respectively. Compared with the data of the clean surface (Fig. 7), the critical angles of the shadowing peaks remain unchanged and no other shadowing arises in the spectrum. This indicates that an Al atom is not located on an atop site nor on a bridge site, but on a threefold-hollow site. The decrease of the peak intensity of the Nb(1)-Nb(1) shadowing at 21.2° is probably due to disturbance of the

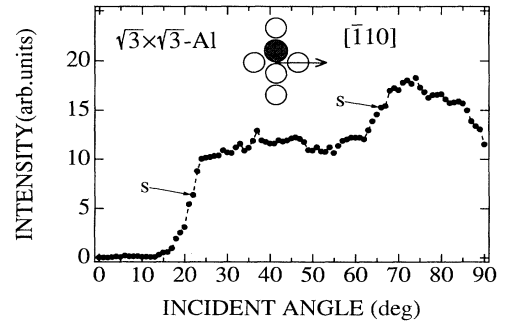

FIG. 8. ICISS spectrum of the Al-adsorbed surface. Solid circles are the experimental data. The dashed line is a guide for the eye. Cf. Fig. 7.

Nb(1) layer caused by Al adatoms. However, the RHEED pattern is as sharp as that of the clean surface. To gain additional information, the surface has been observed by LEED.

Figure 9(a) shows the LEED pattern of the $(\sqrt{3}\times\sqrt{3})R30°$ Al surface. When the incident energy of the electron is lowered, satellite spots appear around main spots [Fig. 9(b)]. The satellite spots indicate six times as long periodicity as the $\sqrt{3}\times\sqrt{3}$ structure in real space. On careful examination, it has been found that the pattern cannot be interpreted by a missing-spot model, so the satellite spots seem to result from the modulated surface structure with three domains. The amplitude of modulation concerning the displacement of the substrate atoms should be small because of the following reasons.

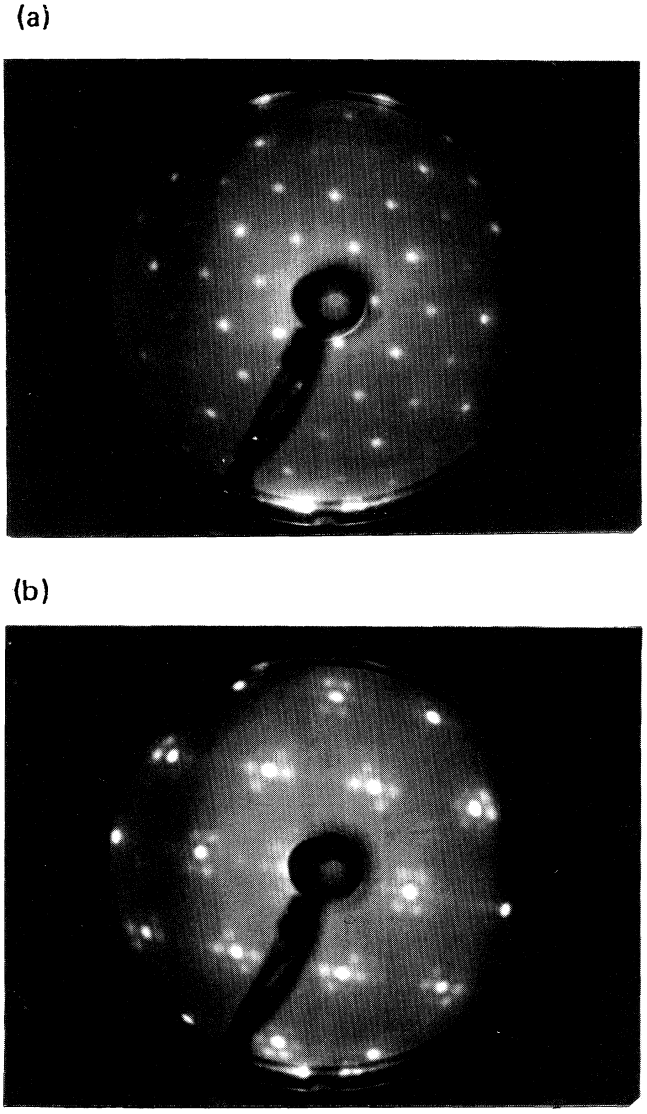

FIG. 9. LEED patterns of the NbC(111) $(\sqrt{3}\times\sqrt{3})R30°$ Al surface. Electron energy is (a) 259 eV, (b) 73.8 eV.

First, the satellite spots can be seen with the 73.8-eV electron energy but hardly seen with 259 eV, which means that the modulation exists in the outer layer in the $\sqrt{3}\times\sqrt{3}$ structure. Second, the angle breadth of Nb(1)-Nb(1) shadowing is larger by 1° than that of the clean surface. This corresponds to a 0.05-Å deviation in the normal direction of the surface. Third, the angle breadth of Nb(1)-Nb(3) shadowing at 70° seems almost the same as for the clean surface. Therefore, the deviation of Nb(1) atoms in the direction parallel to the surface must be less than 0.05 Å.

To ascertain the Al position, the ICISS measurement has been successively performed in the $[\bar{1}\,\bar{1}2]$ and $[11\bar{2}]$ directions.

Figure 10 shows the ICISS spectrum in the $[\bar{1}\,\bar{1}2]$ direction. Compared with the clean surface (Fig. 6), a new shadowing appears at 45.4° and a new blocking at 87.5°. These can be attributed to the Al adatom on the threefold-hollow site above the Nb(3) atom. The shadowing arises from Al-Nb(1) pairs and the blocking is caused by Al atoms obstructing Li^+ ions scattered by Nb(1). It must be noticed that the shadowing at 13.9° is still visible after Al absorption. This indicates that all the threefold-hollow sites are not occupied. The intensity of the ICISS spectrum is proportional to the density of atoms which are visible to the incident beam. Taking account of the correction of the intensity depending on the incidence angle, the ratio of the density of the Nb(1)-Nb(1) pair to the Al-Nb(1) pair is evaluated at about 1:2 in Fig. 10. Consequently, it is concluded that the coverage of Al atoms is two thirds of the Nb monolayer.

Figure 11 shows the ICISS spectrum in the $[11\bar{2}]$ direction. Compared with the clean surface (Fig. 4), it can be seen that a new blocking appears at 55.1° and a

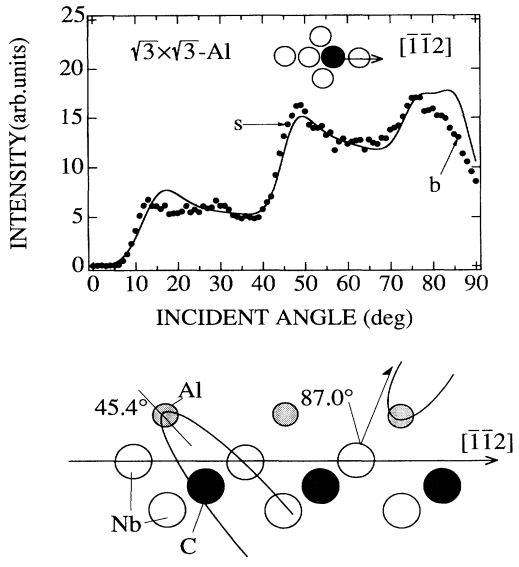

FIG. 10. ICISS spectrum of the Al-adsorbed surface. Solid circles are the experimental data and the solid line is the calculation. *s* means shadowing and *b* means blocking effect caused by Al adatoms. Cf. Fig. 6.

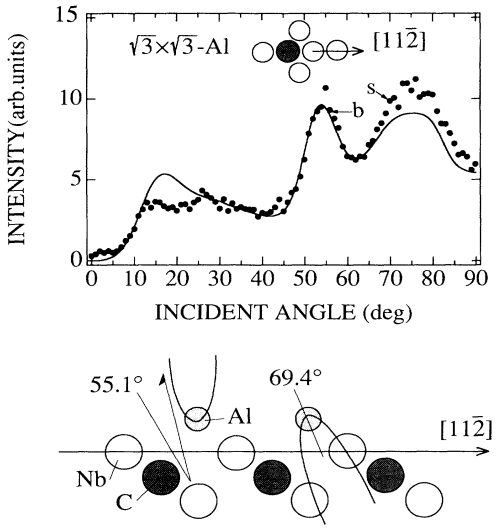

FIG. 11. ICISS spectrum of the Al-adsorbed surface. Solid circles are the experimental data and the solid line is the calculation. *s* means shadowing and *b* means blocking effect caused by Al adatoms. Cf. Fig. 4.

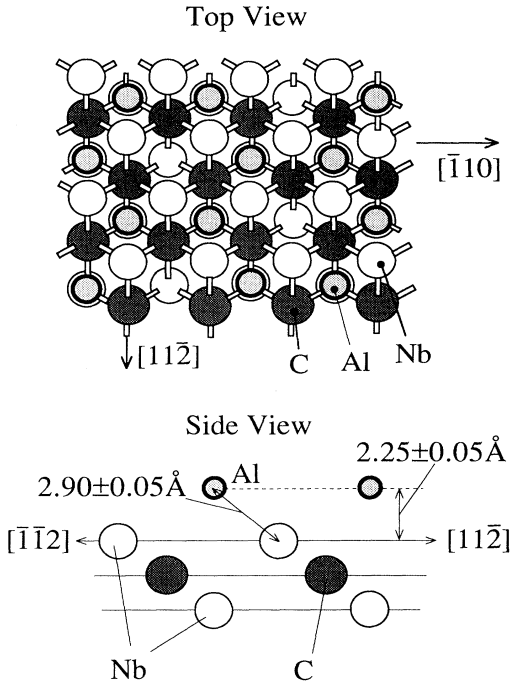

FIG. 12. Schematic view of the NbC(111) ($\sqrt{3}\times\sqrt{3}$)R30° Al surface. Top and side view.

new shadowing peak at 69.4°. These can be completely explained by the same model used for the [$\bar{1}\,\bar{1}$2] direction. The cause of the blocking at 55.1° is that Li^+ ions scattered by Nb(3) atoms are prevented by Al atoms from going out of the surface. The new shadowing at 69.4° arises from Al-Nb(1) pairs.

Computer simulations have been performed to find the configuration of atoms which gives the best fitting curve to the ICISS spectra in both [$\bar{1}\,\bar{1}$2] and [11$\bar{2}$] directions. The solid lines along the experimental data in Figs. 10 and 11 are the best-fitted curve and they show that the Al atom is adsorbed on the threefold-hollow site above the Nb(3) atom with two-thirds monolayer coverage, and the height of it from the surface is 2.25±0.05 Å (Fig. 12). The structure with two-thirds monolayer coverages makes a honeycomb pattern. The relaxation of Nb(1) and C(2) observed in the clean surface remains on the Al-adsorbed surface. Then, the Al-Nb(1) distance becomes 2.90±0.05 Å. In the case of alloys such as Al_3Nb, $AlNb_2$, and $AlNb_3$, the Al-Nb distance is 2.884 to 2.900 Å. These values are close to our result, so that Al-Nb bonding at the NbC(111) surface is considered to be similar to that in the Al-Nb alloy.

Oxygen, nitrogen, and deuterium atoms are adsorbed on the same site with Al. According to the theoretical work about the TiC(111) surface,[5] a Ti atom on the first layer projects its dangling bond toward the center of the threefold-hollow site. This situation must be true on the NbC(111) surface because the electronic structure of group-IV and group-V TMC's are explained by a rigid-band model. These dangling bonds seem to dominate the adsorption process for most kinds of atoms. When Al is adsorbed on the threefold site, three dangling bonds of Nb and three valence electrons of Al combine. Therefore, it is expected that the Al-adsorbed NbC(111) surface is relatively inert compared with the clean surface. In fact, oxygen atoms are desorbed at a temperature below 900 °C from the NbC(111)-Al surface while they are desorbed at about 1400 °C from the clean surface. The site for an O atom is probably the threefold-hollow site which does not have an Al atom. In that case, O-Nb bonding is considered to be weakened by Al adatoms. Another possible cause of the inactivity of the Al-adsorbed surface is that O_2 may be adsorbed as a molecule, so that they are desorbed easily at low temperature. Further investigations are required to determine which model is appropriate.

IV. SUMMARY

The NbC(111) clean surface has a 1×1 unreconstructed structure and the outermost layer is terminated by Nb atoms. The first-layer Nb atoms relax inward by 0.20±0.05 Å and the second-layer C atoms by 0.05±0.05 Å.

On the NbC(111)($\sqrt{3}\times\sqrt{3}$)R30° Al surface, Al atoms are adsorbed on the threefold-hollow site, under which a third-layer Nb atom exists. The coverage is two-thirds monolayer, so Al atoms make a honeycomb pattern. The height of an Al atom from the surface is 2.25±0.05 Å, and the Al-Nb distance is 2.90±0.05 Å. This value is close to that in Al-Nb alloys. On the Al-adsorbed surface, the relaxation of Nb and C atoms remains as on the clean surface.

[1]L. E. Toth, *Transition Metal Carbides and Nitrides* (Academic, New York, 1971).
[2]E. K. Storms, *The Refractory Carbides* (Academic, New York, 1964).
[3]H. Ihara, M. Hirabayashi, and H. Nakagawa, Phys. Rev. B **14**, 1707 (1976).
[4]B. M. Klein, D. A. Papaconstanspoulos, and L. L. Boyer, Phys. Rev. B **22**, 1946 (1980).
[5]T. Hoshino and M. Tsukada, J. Magn. Magn. Mater. **31-34**, 902 (1983).
[6]P. Bhana, J. Redinger, and K. Schwarz, Phys. Rev. B **31**, 2316 (1985).
[7]E. Wimmer and A. Neckel, Phys. Rev. B **31**, 2370 (1985).
[8]S. Kim and R. S. Williams, J. Phys. Chem. Solids **49**, 1307 (1988).
[9]G. H. Schadler and R. Monniner, Z. Phys. B **76**, 43 (1989).
[10]J. Roth, J. Bondansky, and A. P. Martinelli, Radiat. Eff. **48**, 213 (1980).
[11]Y. Ishizawa, S. Aoki, C. Oshima, and S. Otani, J. Phys. D **22**, 1763 (1989).
[12]R. B. Levy, in *Advanced Materials in Catalysis,* edited by J. J. Burton and R. L. Garten (Academic, New York, 1977).
[13]T. Aizawa, Y. Hwang, W. Hayami, R. Souda, S. Otani, and Y. Ishizawa, Surf. Sci. **260**, 311 (1992).
[14]Y. Hwang, T. Aizawa, W. Hayami, S. Otani, Y. Ishizawa, and S. Park, Surf. Sci. **271**, 299 (1992).
[15]M. Hammar, C. Törnevik, J. Rundgren, Y. Gauthier, S. A. Flodström, K. L. Håkansson, L. I. Johansson, and H. Håglund, Phys. Rev. B **45**, 6118 (1992).
[16]K. Miura, R. Souda, T. Aizawa, C. Oshima, S. Otani, and Y. Ishizawa, J. Vac. Sci. Technol. A **7**, 3013 (1989).
[17]G. R. Gruzalski, S.-C. Liu, and D. M. Zehner, Surf. Sci. Lett. **239**, L517 (1990).
[18]P. A. P. Lindberg, L. I. Johansson, J. B. Lindström, P. E. S. Persson, D. S. L. Law, and A. N. Christensen, Phys. Rev. B **36**, 6343 (1987).
[19]K. Edamoto, T. Anasawa, E. Shiobara, M. Hatta, E. Miyazaki, H. Kato, and S. Otani, Phys. Rev. B **43**, 3871 (1991).
[20]S. Otani, T. Tanaka, and Y. Ishizawa, J. Cryst. Growth **62**, 211 (1983).
[21]M. Aono and R. Souda, Jpn. J. Appl. Phys. **24**, 1249 (1985).
[22]G. Moliére, Z. Naturforsch. A **2**, 133 (1947).
[23]O. B. Firsov, Zh. Eksp. Teor. Fiz. **33**, 696 (1958) [Sov. Phys. JETP **6**, 534 (1958)].
[24]R. S. Williams, M. Kato, R. S. Daley, and M. Aono, Surf. Sci. **225**, 355 (1990).
[25]D. J. O'Conner and R. J. MacDonald, Radiat. Eff. **34**, 247 (1977).
[26]S. H. Overbury and D. R. Huntley, Phys. Rev. B **32**, 6278 (1985).
[27]W. Hayami, R. Souda, T. Aizawa, S. Otani, and Y. Ishizawa, Surf. Sci. **276**, 299 (1992).

(a)

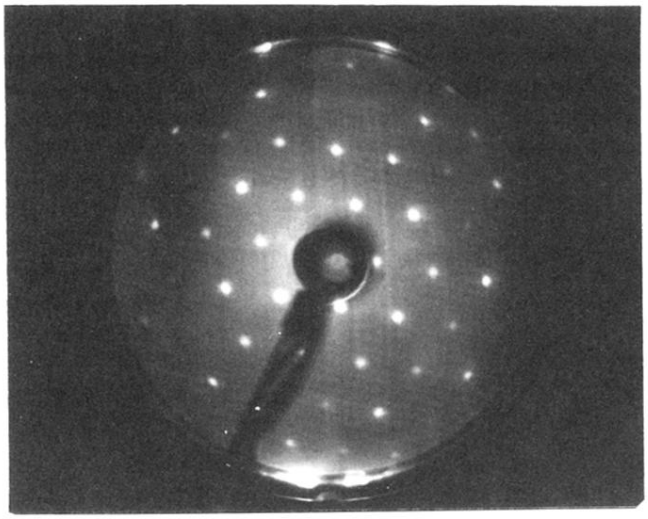

(b)

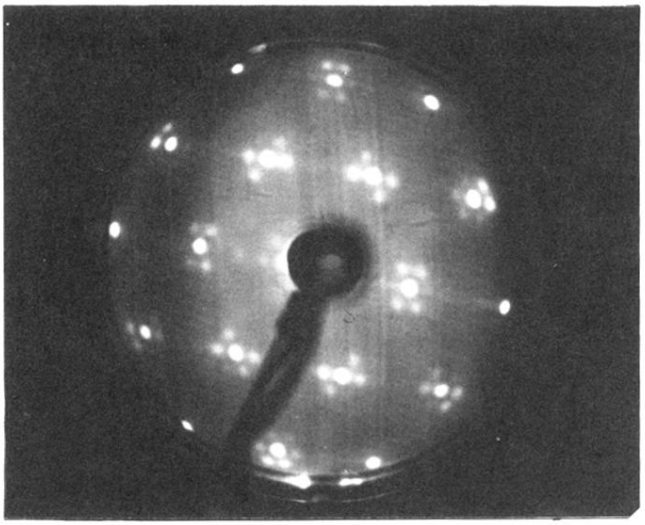

FIG. 9. LEED patterns of the NbC(111) $(\sqrt{3}\times\sqrt{3})R30°$ Al surface. Electron energy is (a) 259 eV, (b) 73.8 eV.